# Correlation of Zero Field Splittings and Site Distortions V. $Mn^{2+}$ in $Cs_2Zn_3S_4$

M. Heming and G. Lehmann
Institut für Physikalische Chemie, Westfälische Wilhelms-Universität, Münster

Z. Naturforsch. **38 a**, 149–153 (1983); received November 15, 1982

*Dedicated to Professor Alfred Klemm on the occasion of his 70th birthday*

In platelets of $Cs_2Zn_3S_4$ with about 4% of the Zn substituted by Mn two nonequivalent centers of isolated $Mn^{2+}$ were observed in addition to a broad EPR signal near $g = 2$ which is assigned to clusters of interconnected $MnS_4$ units. The fine structure and hyperfine structure parameters for the single-ion centers (all in units of $10^{-4}$ $cm^{-1}$) are:

$b_2^0 = -318.3 \pm 3$; $b_2^2 = -210.3 \pm 2$; $A_y = -62.7$; $A_z = -63.6 \pm 0.8$;
$b_2^0 = -890 \pm 18$; $b_2^2 = -743 \pm 36$; $A_y = -60.6$; $A_z = -61.4 \pm 0.8$;

for centers I and II, resp. Center II arises from Zn sites of $C_2$ site symmetry while for center I assignment to either one of two sites with $D_2$ site symmetry is possible. The larger hyperfine splitting constants as well as the superposition analysis favor the larger sites which are not occupied by Zn, but are partly occupied in the analogous Mn (and Co) compounds. Superposition analysis yields the same value of $+0.12 \pm 0.02$ $cm^{-1}$ for the intrinsic zero field splitting parameter $\overline{b_2}$ of the bridging $MnS_4$ units in both sites. $g_z$ is significantly higher than the free ion value indicating a higher degree of covalency than in CdS and $CdGa_2S_4$.

## Introduction

Recently the superposition model [1] has been successfully applied to the second order zero field splitting (ZFS) parameters of the $d^5$-ions $Mn^{2+}$ and $Fe^{3+}$ in a number of cases [2–6]. Especially in cases of lower than axial site symmetry where the principal axes of the fine structure tensor are no longer fixed by symmetry a comparison of the angular variation of the splitting with that calculated from the distortion of the first coordination sphere can serve as a very lucid test of the validity and the possible limitations of this model provided the accuracy of the crystal structure data is significantly higher than the deviations from cubic symmetry, and host and impurity ion are of the same valence and of very similar size so that effects of local lattice relaxation around the paramagnetic impurity remain sufficiently small. The success of this model in such cases indicates that the zero field splittings of these ions are largely dominated by mechanisms which are confined to their first coordination shells, in contrast to electrostatic models which predict sizeable contributions from more distant ions.

Reprint requests to Prof. G. Lehmann, Institut für Physikalische Chemie, Westf. Wilhelms-Universität, Schlossplatz 4, D-4400 Münster.

Increasingly positive values of the intrinsic ZFS parameters (i.e. the ZFS splittings per unit distortion) were found for $Mn^{2+}$ with increasing atomic number of the halide ligands [7]. Comparable data for chalkogenides and pnictides as ligands are still largely missing, partly due to lack of sufficiently accurate crystal structure data.

As part of a systematic investigation aiming at a test of the limitations of the superposition model and (in cases of its applicability) at the determination of the intrinsic ZFS parameters for different ligands we here report data for $MnS_4$ units of distorted tetrahedral symmetry where the sulfide ligands are bridging between two or more divalent metal ions. Previously, a marked difference between bridging and nonbridging fluoride ligands was observed in one case [3]. A crystal structure refinement as well as details of the crystal growth procedure for the host compound $Cs_2Zn_3S_4$ were recently reported [8], comparable data for the analogous manganese compound are also available [9]. Due to occupation of sites of different symmetry by the divalent metal ions – an orthorhombic site of $D_2$ and at least one monoclinic one of $C_2$ point symmetry – this structure appears to be particularly well suited for a test of the model since its validity requires consistent results to be obtained for both sites. Furthermore, due to the layer structure any direct influences of the next-

0340-4811 / 83 / 0200-0149 $ 01.3 0/0. – Please order a reprint rather than making your own copy.

Table 1. EPR parameters of $Mn^{2+}$ in $Cs_2Zn_3S_4$.

| | Center I (4a) | | | Center II (8 g) | | |
|---|---|---|---|---|---|---|
| $b_2^0$ | $-318.5 \pm 3.2$[a] | | | | $-890 \pm 18$ | |
| $b_2^2$ | $-210.3 \mp 2.1$ | | | | $-743 \pm 36$ | |
| $i$ | $x$ | $y$ | $z$ | $x$ | $y$ | $z$ |
| axes | $// a$ | $// b$ | $// c$ | $// b$ | $\pm 35°$ from $c$ | $\pm 35°$ from a[b] |
| $A_i$ | – | $-62.7$ | $-63.6 \pm 0.8$ | – | $-60.6$ | $-61.4 \pm 0.8$[a] |
| $g_i$ | 2.003 | 2.004 | $2.011 \pm 0.005$ | 2.002 | 2.003 | $2.007 \pm 0.003$ |

[a] $A_i$ and $b_2^q$ in units of $10^{-4}$ cm$^{-1}$.
[b] $y$ and $z$ in the $ac$ plane.

nearest neighbor divalent cations are confined to the plane of these layers.

## Experimental

Crystal platelets of a light pink color with about 4% of the Zn substituted by Mn were used. The orientations of the $a$- and $b$-axes in the plane of the layers were determined by X-ray precession photographs. EPR measurements were performed on a commercial Q-band spectrometer at room temperature, details of the experimental procedure and the evaluation of numerical data were previously reported [2], [10]. Since the crystals are sensitive against humidity and air, they were handled in a glove box under dry nitrogen and were completely covered with the glue UHU-hart (UHU-Vertrieb GmbH, D-7580 Bühl) during the measurements.

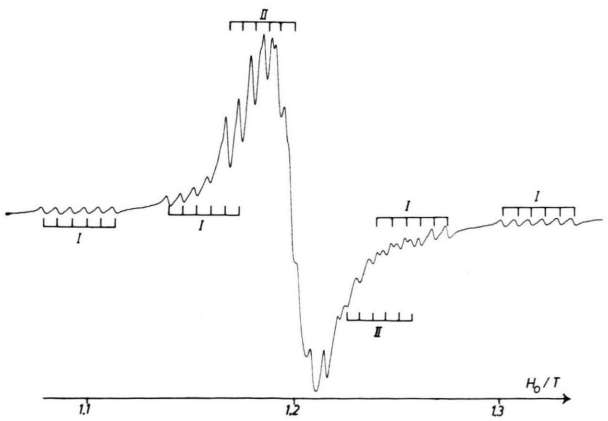


Fig. 1. EPR spectrum of $Mn^{2+}$ in $Cs_2Zn_3S_4$ at 33.69 GHz and room temperature for $H_0 // b$. In addition to the broad central signal due to $MnS_4$ clusters sextets due to centers I and II are clearly resolved at this orientation.

## Results

In Fig. 1 an EPR spectrum for $H_0 // b$ is shown. The broad ($H_{pp}$ 30 to 50 mT) and isotropic signal near $g = 2$ indicates the presence of a large proportion of the $Mn^{2+}$ in clusters of magnetically interacting ions. In addition narrower sextets due to two crystallographically inequivalent centers of isolated $Mn^{2+}$ are also visible. They are labelled I and II. For rotation around the $c$-axis, center II could only be observed for orientations with the $b$-axis approximately along the magnetic field, whereas for rotations around the $b$-axis both centers could be identified. The fine structure parameters, hyperfine splitting constants, $g$-factors and orientations of magnetic axes are given in Table 1. Due to the intense broad signal reliable values for $A_x$ could not be obtained, but they are expected to be intermediate between $A_z$ and $A_y$, the values for maximum elongation and compression, resp. [11]. Thus they should fall within the limits of error of these extreme values.

## Discussion

Apparently center II with noncoincidence of the magnetic $z$- and $y$-axes with crystal axes and presence of two magnetically inequivalent centers symmetrically displaced from the $a$- and $c$-axes is of lower site symmetry and can thus be identified with $Mn^{2+}$ on 8 g sites of $C_2$ point symmetry. The results of a superposition analysis with $t_2 = 7$ and $R_0 = 246$ pm for the crystal $a - c$ plane are shown in Fig. 2; for the splitting diagram a value of $\bar{b}_2 = +0.12$ cm$^{-1}$ is used. There is a very good agreement in the positions of calculated and experimental $z$- and $y$-axes and a good overall agreement in the absolute values for both curves with this choice of $\bar{b}_2$, but

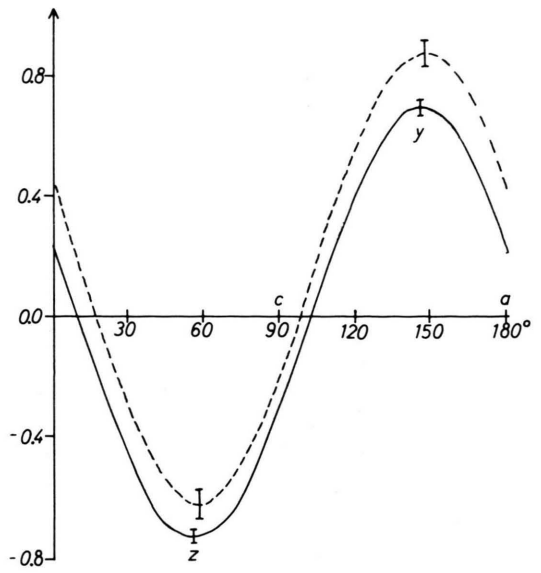


Fig. 2. Comparison of measured (——) and calculated (– – –) angular variation of the zero field splitting of center II in the $a-c$ plane. The measured curve ("splitting diagram") is given by

$$1/2\overline{b_2}\,(3\cos^2\vartheta - 1)\,b_2^0 - \sin^2\vartheta\cdot b_2^2)\,,$$

where $\vartheta$ is the angle between $H_0$ and the magnetic $z$-axis. The calculated curve ("distortion diagram") is given by

$$\tfrac{1}{2}\sum_i (3\cos^2\Theta_i - 1)\,(R_0/R_i)^7\,,$$

with $\Theta_i$ the angle between the $MnS_i$ vectors and the particular directions and $R_0 = 246$ pm. The numbers on the ordinate have the obvious meaning of "effective additional fractional ligand at normal distance". Only one of the magnetically nonequivalent centers is shown.

small differences remain for all orientations outside the limits of error of both EPR and crystal structure data (indicated by bars along the $z$- and $y$-axes). Thus this figure suggests that the $Mn^{2+}$ undergoes less compression in the $ac$ plane than indicated by the crystal structure data for $Zn^{2+}$. However, a complete agreement can always be obtained for any desired direction by a suitable choice of $\overline{b_2}$, and for sufficiently low site symmetries the overall agreement is also somewhat dependent on the choice of the values for the exponent $t_2$ and the normal Mn-X distance $R_0$. The values of $b_2$ required for complete agreement along the $z$- $y$- and $x$-axes, resp. (with the above choice of $t_2 = 7$ and $R_0 = 246$ pm) are $+0.142$; $+0.094$ and $-0.03$ cm$^{-1}$, resp.; the change in sign for the $x$-direction results from the fact that according to the crystal structure data the magnetic $y$-axis (not the $z$-axis) is the direction of maximum distortion. But since $\overline{b_2}$ is the ratio of the experimental splitting and a number derived from crystal structure data, a larger weight must be placed on the values derived for the directions of maximum compression and elongation.

Center I can arise from occupation of either one of two geometrically different sites with $D_2$ site symmetry. As shown in Table 2, Zn exclusively occupies one type (called 4 b) while in the analogous $Cs_2Mn_3S_4$ Mn also occupies the second site 4 a partly [9]. The superposition analysis for center I in Fig. 3 is not consistent with Mn in 4 b sites because large differences between measured and calculated distortions along all three crystal axes (which coincide with the magnetic axes) result: While the largest splitting ($z$-axis) is found to coincide with the crystal $c$-axis, for site 4 b the smallest splitting (i.e. the magnetic $x$-axis) is predicted from the crystal structure data for this axis. Thus for this site all axes would be interchanged. In view of the very similar sizes of $Zn^{2+}$ and $Mn^{2+}$ and the nearly perfect agreement for the 8 g sites it is very unlikely that effects of local lattice relaxation around the Mn impurities are

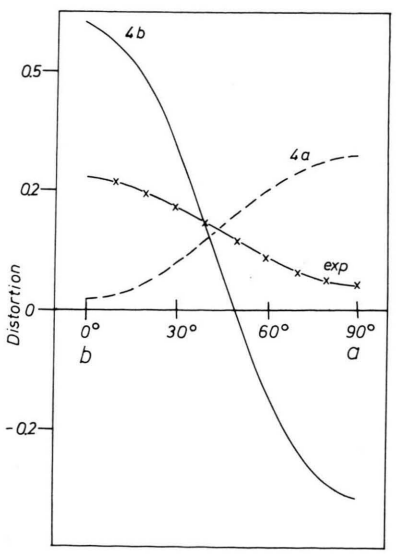


Fig. 3. Comparison of the measured angular variation of the zero field splitting for center I (×——×——×) with those calculated for sites 4a (– – –) and 4b (——) for rotation around the $c$-axis (the magnetic $z$-axis). For the meaning of the numbers on the ordinate see Figure 2. Since this is a rotation from $y$ to $x$, the experimental curve in this case is given by $-(b_2^0 + \cos 2\varphi\cdot b_2^2)/2\overline{b_2}$ where $\varphi$ is the angle to the $b$ (the magnetic $y$) axis.

Table 2. Comparison of crystal structure data for $Cs_2Zn_3S_4$ (1) and $Cs_2Mn_3S_4$ (2).

| Site | 1 | | 2 | | |
|---|---|---|---|---|---|
| | Occupation number | bond length/pm | Occupation number | bond length/pm | Difference/pm |
| 8 g | 8 | 243.9/233.7 | 7 | 241/252 | +8 |
| 4a | 0 | 258.3 | 1 | 254 | −4 |
| 4b | 4 | 236.5 | 4 | 245 | +8 |

responsible. On the other hand, for site 4 a the $z$-axis is correctly predicted by the crystal structure data, but the $x$- and $y$-axes are evidently still interchanged. With the value $\overline{b_2} = 0.12\ cm^{-1}$ previously obtained for the 8 g sites the agreement along the $c$-axis is practically perfect, but the geometry in the $ab$ plane seems to differ significantly from that for the pure $Cs_2Zn_3S_4$. We attribute at least the larger part of these differences to the fact that occupation of a normally empty (i.e. interstitial) site should change its immediate surroundings considerably.

Two additional facts support assignment of center I to the 4 a sites:

a) The average Zn−S distance for site 4 b is considerably smaller than for the other sites (see Table 2). It is known that larger impurity ions preferentially occupy the larger lattice sites of a particular host ion. Examples are $Fe^{3+}$ in $Al_2BeO_4$ [12] and $Al_2SiO_5$ (cyanite) [13], [14]. Also, in $NaNO_3$ and KCl a marked decrease of the distribution coefficients of larger alkali ions with increasing size was observed [15]. An occupation ratio of 20 between sites 4 a and 4 b would be sufficient to obscure presence of $Mn^{2+}$ in 4 b sites for the signal/noise ratios of our EPR measurements. This would require site preference energies between 25 and 30 kJ/mol for growth temperatures between 1000 and 1200 K. These are larger than the values calculated from the data for KCl and $NaNO_3$ for similar differences in size, but clearly these systems are too different to allow direct comparisons.

b) The hfs splitting constants $A_i$ for center I are markedly larger than for center II and thus indicate a larger average Mn−S distance for center I [11]. This is compatible only with site 4 a, for site 4 b smaller values should result.

Thus while none of these observations can be regarded as an undisputible proof, they all support identification of center I with $Mn^{2+}$ in 4 a sites. For mixed crystals $Cs_2Zn_xMn_{3-x}S_4$ with $x$ near 1.5, however, exclusive occupation of sites 4 b by both Zn and Mn is indicated by neutron diffraction data [16]. Thus the distribution of Mn among the 4 a and 4 b sites seems to vary in a complicated way depending on the Zn/Mn ratio. In our crystals a higher tendency of $Mn^{2+}$ on 4 b sites for cluster formation may just feign a low occupation ratio for this site.

The axial fine structure parameter $b_2^0$ for $Mn^{2+}$ in $CdGa_2S_4$ [17] is also compatible with our value of $0.12\ cm^{-1}$, but the available crystal structure data [18] are not accurate enough to allow a conclusive test. If we take the slightly different coordinates for sulfur proposed in recent EPR work on $Fe^{3+}$ in this compound [5], a value of $\overline{b_2} = +0.12\ cm^{-1}$ for $Mn^{2+}$ is also obtained. The Cd−S distance of 243.7 pm resulting with these parameters, however, appears to be too short from consideration of the size of $Cd^{2+}$ and the value for the hfs constant A of $-64 \cdot 10^{-4}\ cm^{-1}$ [17], slightly larger than in $Cs_2Zn_3S_4$.

Practically the same value of $\overline{b_2}$ was also obtained for $Mn^{2+}$ in ZnO [7], but this is based on crystal structure data [19] of rather limited accuracy. Judging from the results for halides as ligands [7] a more positive value would be expected for sulfur compared to oxygen as ligand.

The remaining differences between splitting and distortion diagrams in Fig. 2 and 3 may at least partly be caused by direct influences of next-nearest neighbors. The fact that these Zn neighbors are confined to the $ab$ planes of the layer structure allows an at least qualitative test of this possibility. For the 8 g sites they should then cause a more negative value of the distortion (i.e. less compression) along $a$ and a more positive one along $b$. The shortest Zn−Zn distances for this site are nearly parallel to the $a$-axis, thus for this site a negative value of $\overline{b_2}$ for Zn would be required to reduce the differences between splitting and distortion diagram. The shortest Zn−Zn distance for the 4 a site acts along the $b$-axis, but here a positive value of $\overline{b_2}$ for Zn would be required to reduce the difference between calculation and experiment. Finally, the 4 b sites have longer Zn−Zn distances so that in this case their influence should not significantly reduce the large differences. Thus unless the local lattice relaxation overcompensates direct influences of the $Zn^{2+}$ for the 4 a site, the lack of perfect agreement cannot be ascribed to

neglect of direct influences of next-nearest neighbors. Like in $BaZnF_4$ [3] they are thus not very likely.

For $Mn^{2+}$ in 4a sites a corresponding number of Zn vacancies in 4b and/or 8g sites should exist. These vacancies could either be associated with the $Mn^{2+}$ ions or randomly distributed in the lattice. The first case can be excluded since it should result in lowering of the site symmetry of Mn which is not observed. Also, more than one center of this kind would be likely depending on the positions of the vacancies. The highly covalent nature of the bonds in this compound significantly reduces the Coulomb attraction between the positive charge of an interstitial divalent manganese and the zinc vacancies with a formally negative charge and thus reduces the free energy of formation of such manganese-vacancy complexes.

*g-factors and covalency*

As shown in Table 1, the $g$-factors for both centers appear to be considerably anisotropic with values for $g_z$ significantly larger than the free electron value. For more ionic systems small and negative $g$-shifts are normally observed. They can be rationalized assuming a small admixture of the excited $^4T_1(P)$ into the ground state [20, 21]. Larger positive $g$-shifts were previously also observed in binary [22] and ternary [17] chalkogenide systems. They can be explained within the MO formalism as a result of covalent admixture of ligand $p$-functions into the metal 3d functions which effectively results in transfer of negative charge from the ligands to the central ion [20, 23]. Since this positive $g$-shift increases from sulfides to tellurides [17, 24], it can be regarded as a rough measure of covalency. The values for $Mn^{2+}$ in $Cs_2Zn_3S_4$ are higher than in binary sulfides and in $CdGa_2S_4$. They thus indicate a higher degree of covalency for the Mn–S bonds in this layer structure than in other compounds with three-dimensional networks.

*Acknowledgements*

We thank Prof. Dr. W. Bronger and Dipl.-Chem. U. Hendriks for supply of the $Cs_2Zn_3S_4$ crystals and for valuable discussions. Support of this work by the Deutsche Forschungsgemeinschaft and by the Fonds der Chemischen Industrie is also gratefully acknowledged.

[1] D. J. Newman and W. Urban, Adv. Phys. **24,** 793 (1975).
[2] M. Heming, G. Lehmann, G. Henkel, and B. Krebs, Z. Naturforsch. **36a,** 286 (1981).
[3] K. Recker, F. Wallrafen, R. Büscher, and G. Lehmann, phys. stat. sol. (b) **107,** 699 (1981).
[4] A. Leblé, J. J. Rousseau, J. C. Fayet, and C. Jacoboni, Sol. State Commun. **43,** 773 (1982).
[5] B. Frick and D. Siebert, Z. Naturforsch. **38a,** 1005 (1982).
[6] M. Heming, G. Lehmann, K. Recker, and F. Wallrafen, phys. stat. sol. (b) (submitted).
[7] M. Heming and G. Lehmann, Chem. Phys. Letters **80,** 235 (1981).
[8] W. Bronger and U. Hendriks, Rev. Chim. Mineral. **17,** 555 (1980).
[9] W. Bronger and P. Böttcher, Z. anorg. allg. Chem. **390,** 1 (1972).
[10] H. Sachs and G. Lehmann, phys. stat. sol. (b) **92,** 417 (1979).
[11] G. Lehmann, J. Phys. Chem. Sol. **41,** 919 (1980).
[12] W. R. Barry and G. J. Troup, phys. stat. sol. **38,** 229 (1970).
[13] G. J. Troup and D. R. Hutton, Brit. J. Appl. Phys. **15,** 1493 (1964).
[14] G. Lehmann, phys. stat. sol. (b) **99,** 623 (1980).
[15] H. Nagasawa, Science **152,** 767 (1966).
[16] W. Bronger, private communication.
[17] M. Schlaak and A. Weiss, Z. Naturforsch. **27a,** 1624 (1972).
[18] H. Hahn, G. Frank, W. Klinger, A.-D. Störger, and G. Störger, Z. anorg. allg. Chem. **279,** 241 (1955).
[19] S. C. Abrahams and J. C. Bernstein, Acta Crystallogr. **B25,** 1233 (1969).
[20] H. Watanabe, Progr. Theor. Phys. **18,** 405 (1957).
[21] J. R. Gabriel, D. F. Johnston, and M. J. D. Powell, Proc. Roy. Soc. London **73,** 116 (1959).
[22] T. P. P. Hall, W. Hayes, and F. I. R. Wilkins, Proc. Phys. Soc. London **78,** 883 (1961); J. Schneider, S. R. Sircar, and A. Räuber, Z. Naturforsch. **18a,** 980 (1963); O. Okada, T. Miyadai, and S. Akimoto, J. Phys. Soc. Japan. **39,** 312 (1975); O. Okada and T. Miyadai, Japan. J. Appl. Phys. **17,** 231 (1978).
[23] I. Fidune and K. W. H. Stevens, Proc. Phys. Soc. London **73,** 116 (1959).
[24] R. S. Title, Phys. Rev. **131,** 623 (1963).